



OPEN The role of anxiety in modulating temporal processing and sensory hyperresponsiveness in autism spectrum disorder: an fMRI study

Takeshi Atsumi^{1,2,5✉}, Masakazu Ide^{2,5}, Mrinmoy Chakrabarty^{3,4} & Yasuo Terao¹

The atypical sensory features and high comorbidity of anxiety disorders in individuals with autism spectrum disorder (ASD) are attracting increasing attention. Among individuals with ASD, those who exhibit heightened sensory hyperresponsiveness tend to show enhanced temporal processing of sensory stimuli, despite no observed differences in stimulus detection thresholds. A previous study reported the role of anxiety in modulating emotion-cued changes of visual temporal resolution in ASD. Building on this, we hypothesized that elevated anxiety might contribute to increased activation of neural circuits for timing perception and sensory hyperresponsiveness. This study included 25 individuals with ASD and 25 typically developed (TD) participants. Using functional magnetic resonance imaging (fMRI), we examined neural activity during a visual temporal order judgment task pre-cued by facial emotions. In the TD group, but not the ASD group, the presence of fearful facial expressions enhanced temporal processing. However, a correlation of anxiety levels with emotion-cued task performance and sensory hyperresponsiveness, respectively, was evident in the ASD group. In the TD group, neuroimaging revealed greater activation of the right caudate compared with that in the ASD group and a functional connectivity between the amygdala and left supramarginal gyrus. Individuals with ASD showed a relationship between anxiety level and activation of the right angular gyrus. Moreover, anxiety mediated the link between right angular gyrus activation and sensory hyperresponsiveness in the ASD group. These findings suggest that enhancement of temporal processing by fear-related cues—reflecting an emotion-timing neural circuit—may be disrupted in individuals with ASD. Heightened anxiety and sensory hyperresponsiveness in ASD may be mediated by brain regions involved in timing perception.

Keywords Autism spectrum disorder, Sensory over-responsivity, Sensory processing, Anxiety, fMRI

Autism spectrum disorder (ASD) is a neurodevelopmental disorder characterized by difficulty in social communication and restricted and repetitive behaviors. It has been reported that approximately 90% of individuals with ASD experience daily sensory challenges such as sensory hyper- and hyposensitiveness¹, so understanding the underlying mechanism is a pressing concern. ASD is also known to show a high rate of comorbidity with anxiety disorders, with estimates ranging from 20% in adults to over 60% in young children^{2,3}. High levels of anxiety enhance the response of the autonomic nervous system to threatening stimuli, resulting in increased arousal⁴. In young patients with ASD, the levels of physiological arousal are correlated with neuroadaptations linked to sensory hyperresponsiveness^{5,6}. These suggest a neurophysiological substrate of the linkage between anxiety and abnormal sensory features in ASD^{7,8}.

Modulation of the autonomic nervous system by emotional signals is mediated by structures in the diencephalon, such as the hypothalamus⁴, which processes sensory inputs. The thalamo-cortico-striatal circuits, including the prefrontal cortex, higher-order motor-related areas, the posterior parietal cortex, and the basal ganglia are considered important for time perception⁹, and decreased levels of the inhibitory neurotransmitter

¹Department of Medical Physiology, Kyorin University, Tokyo, Japan. ²Department of Rehabilitation for Brain Functions, Research Institute of National Rehabilitation Center for Persons with Disabilities, Saitama, Japan.

³Department of Social Sciences and Humanities, Indraprastha Institute of Information Technology Delhi (IIIT-D), Delhi, India. ⁴Centre for Design and New Media, Indraprastha Institute of Information Technology Delhi (IIIT-D), Delhi, India. ⁵Takeshi Atsumi and Masakazu Ide contributed equally to this work. ✉email: atsumi-takeshi@ks.kyorin-u.ac.jp

gamma-aminobutyric acid (GABA) in the circuits, such as the left ventral premotor cortex¹⁰ and the thalamus¹¹, may be linked to increased subjective sensory hyperresponsiveness in ASD. It has also been reported that individuals with ASD exhibit increased sensory hyperresponsiveness and greater accuracy in the tasks demanding timing perception^{12,13}. No associations are reported in the literature between simpler detection tasks and sensory hyperactivities in ASD^{12–14}. This suggests that cognitive functions involved in daily sensory issues in autism may be limited. Many studies have shown that brain regions and functions of neurotransmitters considered to be involved in timing and time perception are distorted in patients with ASD (e.g.¹⁵). . . Abnormal interval timing including the temporal order judgment (TOJ) task in ASD has also been suggested by a meta-analysis¹⁶. Studies also indicate that increased brain circuit excitability, in terms of information processing cycles per unit time⁹, is associated with sensory hyperactivity in ASD^{10,11}. It could be assumed that increased activation of the brain circuits for timing is associated with extraordinarily high perceptual processing cycle and result in frequent experience of sensory hyperactivity¹³. Our previous research demonstrated that the presentation of a disgust-relevant facial expression enhances the accuracy of the TOJ task in individuals with ASD but not in typically developed (TD) individuals, and that this effect is associated with anxiety level¹⁷.

Based on these findings, we hypothesized that abnormal responses in neural circuits related to timing perceptions are associated with the daily sensory challenges and increased anxiety in individuals with ASD. Autistic individuals with high-level anxiety would exhibit a greater response in timing and emotion-related regions by a task-irrelevant negative emotion stimulus, and the neural signal change should be associated with enhanced timing performance and hyperresponsiveness regarding daily sensory experiences. In this study, we investigated the unique neural correlations in ASD regarding the modulation of temporal processing (TOJ) by the presentation of emotion-related stimuli. We used functional magnetic resonance imaging (fMRI) to analyze the effects of presenting fear-relevant face images, which are known to have a strong relationship with activation of the amygdala, a key region for emotional processing^{18,19}. We hypothesized that neural activation in timing-related circuits would enhance the sensory hyperactivity mediated by anxiety and its engagement with the amygdala. The amygdala has multiple projections, including the basal ganglia and the inferior parietal cortex²⁰. These regions are thought to be involved in timing perception (for a review, see⁹). Since we predicted that the performance of the TOJ would be improved by activation at the network level, we performed whole-brain and functional connectivity analyses.

Methods

Participants

This study was reviewed and approved by the ethics committee of Kyorin University and the National Rehabilitation Center for Persons with Disabilities, and was conducted in accordance with the Declaration of Helsinki and the guidelines for human research of both institutes. We recruited 29 ASD and 27 TD participants for the present study at Kyorin University and the Research Institute of National Rehabilitation Center for Persons with Disabilities, through the laboratory website. Some participants were excluded through screening (as described below), and the final sample included 25 individuals with ASD (16 female participants, mean [\pm SD] age 25.28 [6.70] years) and 25 TD individuals (19 female participants, 23.88 [6.77] years). In the final sample, 6 female participants with ASD had attention-deficit/hyperactivity disorder (ADHD) and 1 female ASD participant had anxiety disorder. None of the TD participants had a diagnosis of a neurodevelopmental or psychiatric disorder. In the final dataset for the ASD population, the intelligence quotient (IQ) of 15 participants was assessed using the Japanese version of the Wechsler Adult Intelligence Scale-Third Edition (WAIS-III), and the IQ of 5 participants was assessed using the Fourth Edition (WAIS-IV). The mean age of the participants who had an IQ score measured using one of the WAIS scales was 26.6 years (range: 16–37 years). The remaining 4 participants (mean age = 17.5 years, range: 16–20 years) were assessed using the Japanese version of the Wechsler Intelligence Scale for Children-Fourth Edition (WISC-IV). Note that the translated versions of the WAIS and WISC have been confirmed for validity and reliability in over 1000 Japanese populations^{21,22}. In the final dataset of the ASD group, one participant with ASD did not have IQ data. Considering this exception, the averaged full-scale IQ across 24 ASD participants was 105.75 (\pm SD = 14.63; range 62–124). One participant exhibited a full-scale IQ of 62 (<75) but was not diagnosed as having any intellectual disability. We administered the Autism Spectrum Quotient (AQ;^{23,24}) to all participants to assess the severity of autism-related traits in the two groups. Demographic data of the present cohort are shown in Table 1.

To assess subjective individual sensory traits, we used the Adolescent/Adult Sensory Profile (AASP;²⁵), which originated from Dunn's model of sensory processing disorders²⁶ based on Ayres' theory of sensory integration²⁷. The AASP is broadly accepted for characterizing daily sensory challenges in individuals with ASD and is a 60-item questionnaire classified into four subscales (normal range): Low registration (23–38), Sensation seeking (30–47), Sensory sensitivity (25–42), and Sensation avoiding (25–41). The first two categories correspond to hyporesponsiveness, and the latter two to hyperresponsiveness to sensory stimuli in daily experiences²⁸. Note that even though the subscales are categorized as corresponding to hyper- or hyporeactivity, they are not exclusive, so the normal range of each scale may overlap.

We assessed the anxiety levels of each subject using the Japanese version of the State-Trait Anxiety Inventory (STAI;²⁹). The STAI consists of 40 questions and evaluates state anxiety, which is a transient situational reaction tendency to anxiety-provoking events, and trait anxiety, which is a relatively stable reaction tendency to anxiety experiences. The Japanese version of STAI has also been validated in the Japanese population³⁰.

Written informed consent to participate in this study was provided by the participants. Because we had confirmed that none of the participants with ASD had been diagnosed with intellectual disability and that they understood the purpose of the present study, we were able to obtain written informed consent from the participants themselves.

Variable	Group		Statistic	Effect size
	TD n = 25	ASD n = 25		
Sex (male: female)	6:19	9:16	Odds ratio = 1.76 ^a n.s.	CI = [0.45, 7.44]
Age	23.88 (6.77)	25.28 (6.70)	$t = -0.74^b$ n.s.	$d = -0.21$ CI = [-0.76, 0.35]
AQ	17.88 (7.07)	34.40 (5.90)		
AASP				
Low registration	32.48 (9.25)	45.44 (8.27)	$t = -5.22^b$ ***	$d = -1.48$ CI = [-2.1, -0.85]
Sensation seeking	41.60 (6.83)	35.68 (7.36)	$t = 2.95^b$ **	$d = 0.83$ CI = [0.26, 1.41]
Sensory sensitivity	36.92 (8.73)	51.36 (12.63)	$t = -4.70^b$ ***	$d = -1.33$ CI = [-1.94, -0.72]
Sensation avoiding	38.48 (9.39)	50.60 (11.37)	$t = -4.11^b$ ***	$d = -1.16$ CI = [-1.76, -0.56]
STAI				
State (Y1)	41.16 (8.05)	47.40 (10.03)	$t = -2.43^b$ *	$d = -0.69$ CI = [-1.26, -0.12]
Trait (Y2)	45.40 (10.31)	60.12 (9.54)	$t = -5.24^b$ ***	$d = -1.48$ CI = [-2.11, -0.86]
	TD n = 25	ASD n = 24		
Full-scale IQ	–	105.75 (range: 62–124)		

Table 1. Demographic data and behavioral results of the cohort. TD: typically developed; ASD: autism spectrum disorder; AQ: Autism Spectrum Quotient; AASP: Adolescent/Adult Sensory Profile; STAI: State-Trait Anxiety Inventory; IQ: intelligence quotient; SD: standard deviation; d : Cohen's d ; CI: 95% confidence interval. Mean (SD) are shown for each group. ^aFisher's exact test. ^bWelch's t -test. n.s. = not significant; * $p < 0.05$; ** $p < 0.01$; *** $p < 0.001$.

Apparatus

To evaluate the temporal processing characteristics of each participant's vision, we used the Inroom Viewing Device (1920 × 1080 resolution, 60 Hz, manufactured by NordicNeuroLab, purchased from Physiotech Co., Ltd.), a display that can be used in the MRI room connected to an experiment controller PC (Vaio, Sony) outside the room. For synchronization with the MRI scanner, we acquired the input from the MR synchronizer (GETS3) connected to the signal output device via a USB connection with the experiment controller PC and synchronized it with the experiment program. A non-magnetic keypad (Uchida Denshi, UDS-2012-4) was used to record each participant's response in the behavioral task. We used PsychoPy (written in Python³¹) for experimental control and stimulus presentation.

Stimuli

In our fMRI analysis, we analyzed the effects of presenting images with two types of facial expressions: fearful face (FE) and neutral face (NE) on a temporal cognitive task performance immediately after presentation. We selected stimuli from the NimStim facial expression database³² and the Amsterdam Dynamic Facial Expression Set (ADFES;³³) that were classified as “fearful” and “neutral.” We intended to present each face image only once to avoid inducing a specific response to one face image, but there were very few faces in each set. Therefore, we merged these two face data sets. Since the latter dataset is a video database, we selected frames of the neutral face at the start of the video and the frame of the high expression intensity of fear in the video as stimulus images for each condition³⁴. The NimStim database has been evaluated psychometrically for validity and reliability for recognition of the emotions of these images in untrained individuals³⁴. The reported mean validities of the open- and closed-mouth fearful and neutral images ranged from 0.47 to 0.73 and from 0.82 to 0.91, respectively. The test–retest reliabilities were 0.68 to 0.75 and 0.86 to 0.94, respectively. Fear face images from the ADFES dataset were found to convey significant negative valence (2.37) relative to the midpoint (3.5) of the emotion rating³³. Since the size of the participant's face area differed from the image size, we used OpenCV Haar Cascades to automatically detect the face and remove unnecessary parts around it.

Procedure

Each participant completed the TOJ task and answered the questionnaires. To reduce physical and psychological stress by limiting the number of trials during fMRI, participants performed the task twice: without the face image

conditions to estimate the temporal resolution threshold (just noticeable difference [JND]) during structural image acquisition and with the face image conditions during fMRI (Fig. 1). First, to measure the temporal processing accuracy (temporal resolution) of each participant, we administered a task while acquiring structural images of the brain before performing fMRI. In the TOJ task, a fixation point was presented at the center of a uniform gray screen, and after a random intertrial interval (ITI) of 1 to 1.5 s, two white circles (diameter visual angle 1°) appeared successively at the top and bottom of the left peripheral field (8° horizontally and 3° vertically from the center, respectively) in a random order. The two stimuli were presented for 16.67 ms with various stimulus-onset asynchronies ([SOAs] $\pm 0, 16.67, 33.33, 50.0, 66.67$ ms). After presentation of the second stimulus, participants were asked to report the subsequent presentation within 3 s by pressing a button on the keypad. Participants completed 100 trials with 10 repetitions of each SOA condition. To calculate the temporal resolution (JND), we fitted a sigmoidal function to the response data using a 4-parameter logistic regression model by the maximum likelihood method, and used the 75% point as the JND. The calculated JND was used as the SOA for the task in the fMRI analysis for each individual, followed by its approximation.

In the fMRI task, participants performed the same task as above under almost identical experimental conditions except as follows (Fig. 1): the experiment was conducted using an event-related design in which images with two different facial expressions were randomly presented immediately before the TOJ-related stimulus on each trial. After 15 s of ITI, a facial image was presented to the center of the monitor triggered by a signal input from the scanner. The images were displayed for a random duration of 300 to 500 ms but adjusted such that the time from scanner signal input to the end of image display was 800 ms. The ITI was immediately inserted after 3 s had passed following the presentation of the second stimulus. Each participant completed a total of 40 trials, comprising 20 trials under each of the FE and NE conditions. After every 20 trials, an additional 15 s was inserted as a resting period.

For this second task, participants were informed that an image would appear immediately before the presentation of the TOJ-related stimulus and were instructed to maintain their gaze on the fixation point while

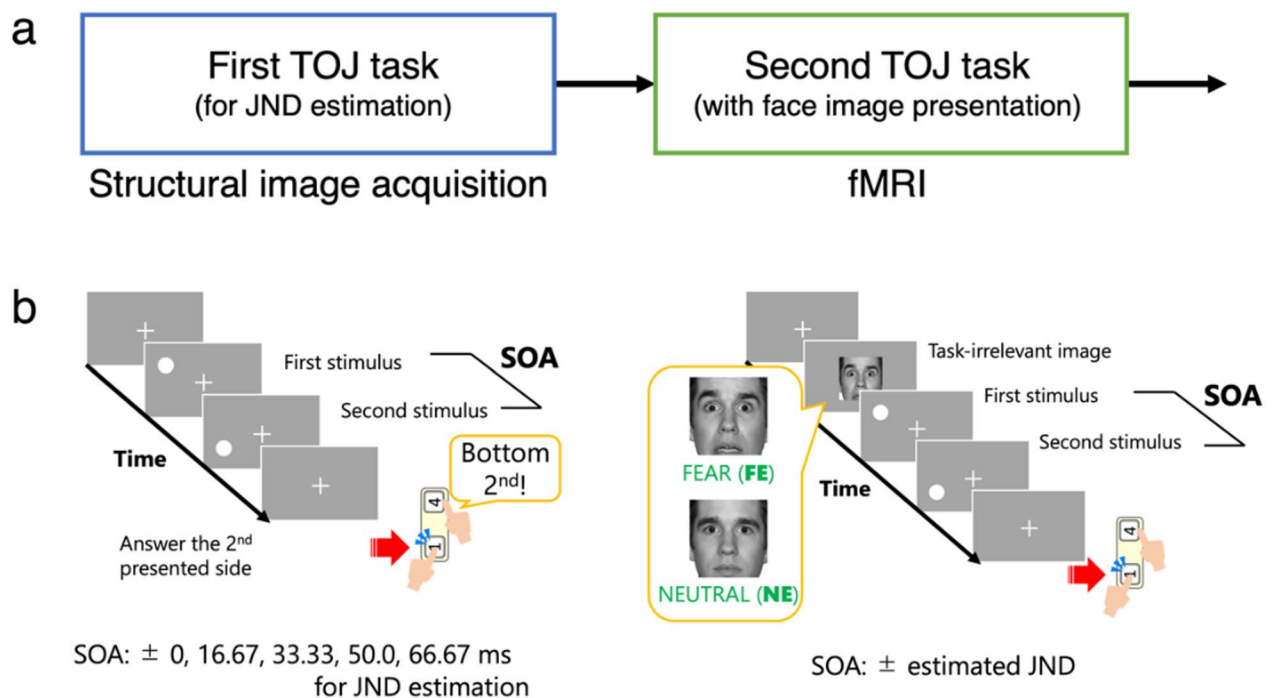


Fig. 1. Schematic image of the experiment. **(a)** The time course of the session. Participants performed the temporal order judgment (TOJ) task during both structural and functional image acquisition. The first performance was used to estimate the individual temporal threshold for the task without face image presentation, and the second was used for the fMRI investigation of the emotion-related image presentation in the task using the estimated near threshold. **(b)** Schematic representation of the TOJ tasks. *Left:* the two stimuli were presented for 16.67 ms with different stimulus onset asynchronies ([SOAs] $\pm 0, 16.67, 33.33, 50.0, 66.67$ ms). Participants had to respond to the top/bottom side of the second presented stimulus. Threshold (just noticeable difference [JND]) was calculated using a function fitted to the response data in each SOA condition before the next task. *Right:* An event-related fMRI of the TOJ task with face presentation. Participants were asked to perform the same task during the structural scan. In each trial, the fear-related (FE) or neutral (NE) face image appeared after an intertrial interval (ITI) and then the task-related stimuli were presented. The percentages of correct responses in the FE and NE conditions were calculated, and the MR signal changes during each condition were analyzed.

ignoring the image as they completed the task. Participants were able to lie supine, hold the keypad, and view the stimulus display outside the scanner via a mirror placed in the head coil.

Image acquisition and processing

MR images were obtained at the National Rehabilitation Center Hospital for Persons with Disabilities using a 3 Tesla Siemens Skyra and a 64-channel head coil. The T1-weighted structural images during the first TOJ task were obtained using MPRAGE (TR=2300 ms, TE=2.98 ms, flip angle=9°, field of view [FoV]=256 mm, voxel size=1 mm³, matrix=256×256, total volume=176 images). Functional images sensitive to the blood oxygenation level dependent (BOLD) contrast³⁵ were obtained from a T2* gradient-echo planar imaging (EPI) pulse sequence (TR=2620 ms, TE=30 ms, flip angle=90°, FoV=281 mm, voxel size=2.2×2.2×3.2 mm³, slice thickness=3.2 mm, slice number=39; interslice gap=1.28 mm, total volume=313 images). The images were preprocessed using SPM12 (<http://www.fil.ion.ucl.ac.uk/spm>) in MATLAB. The functional images of the experimental session (i.e., run) were realigned, slice time was adjusted; mean functional image of each session was coregistered to the structural image, spatially normalized to standard T1-template image defined by the Montreal Neurological Institute (MNI), and spatially smoothed with a Gaussian kernel of 8-mm full-width at half-maximum. The preprocessed data from each subject was analyzed using the generalized linear model (GLM) to examine the effects of the face conditions for each subject based on the previous study³⁶. Data were first entered into fixed effect analysis where task-related neural activity relative to baseline was modeled using a boxcar function, convolved using a canonical hemodynamic response function and filtered by the high-pass filter with a cutoff period of 128 s to rule out low-frequency trends. In the first level analysis for each participant, T-contrast was defined for the FE>NE comparison. The six head motion parameters estimated earlier were regressed out as covariates of no interest in the contrast. MRI data from ASD participants may be blurred by, for example, head motions because of pathological characteristics of the aberrant motor functions³⁷. We thus applied the toolbox for artifact repair (ArtRepair toolbox) implemented on SPM. The subsequent group analyses were carried out using these individual data.

Group analysis

Behavioral data

Group comparisons of behavioral and psychological data were examined using Welch's *t*-test. The correlations across the data were tested using Pearson's product-moment correlation coefficient. The group and the face condition effects for the task performance during fMRI were examined by using a generalized linear mixed model (GLMM)-based analysis of variance (ANOVA). The specific statistical analyses of behavioral data were performed using R ver. 4.1.2 (<http://www.R-project.org>), and the lmerTest function modeling the participant ID as the random effect was used for the GLMM-based ANOVA.

Imaging data

The group comparison and multiple regression analyses for the behavioral and psychological data in each group were examined by whole-brain analysis using SPM12. Functional connectivity in each group was assessed by the psychophysiological interaction (PPI) analysis implemented in SPM. We used the bilateral amygdala as the seed region to test the effect of the FE condition on the TOJ task based on the strong a priori hypothesis of the amygdala response to fear-relevant images^{18,19}. The seed regions of interest were defined using the anatomical mask³⁸ generated by Wake Forest University PickAtlas Toolbox^{39,40} and its embedded Automated Anatomical Labeling (AAL⁴¹). Voxels reported as significant in all group-level results were those that survived an initial height threshold of $p < 0.001$, uncorrected at voxel level ($Z > 3.09$) to isolate clusters, and $p < 0.05$, family wise error (FWE)-corrected for multiple comparisons at the cluster level, excepting the marginally significant correlation between the right angular gyrus and STAI total score in the ASD group ($p_{\text{FWE}} = 0.057$; see “Results” section). To examine the effect of the specific BOLD signal change associated with individual anxiety levels on sensory hyperresponsiveness, we performed the causal mediation analysis⁴² using a R package, mediation⁴³. For labeling the brain area of peak coordinates, Anatomy toolbox⁴⁴ was used. Areas not reported by this source were identified by MRICron (<https://www.nitrc.org/projects/mricron>). Brodmann areas (BAs) were labeled using mni2tal (<https://bioimagesuiteweb.github.io/webapp/mni2tal.html>)⁴⁵. Statistical values were transformed into Z-values and visualized by superimposition on the MNI152 template by using MRICroGL (<https://www.nitrc.org/projects/mricrogl/>).

Exclusion criteria

We excluded participants who did not have sufficient visual acuity (0.1 or more) or who could not distinguish the facial expressions. Visual acuity for each participant was self-reported. We also excluded participants who met the malfunction of the response keypad could not perform the TOJ task during fMRI (average correct performance of the two face conditions < 50%), or who lacked behavioral, psychological (STAI/AASP), or imaging data. For the group comparison of the imaging data, we applied a motion outlier test in the ASD group for motion correction⁴⁶. We used an implemented function of ArtRepair toolbox to detect the group outlier for a between-group comparison (see “Results” section). We performed the outlier detection of ArtRepair examining the global quality metrics for a contrast image from all participants in the ASD group⁴⁷. Using the fMRI data, the distribution of contrast estimates over the brain was calculated to obtain the global quality mean and standard deviation for each participant. One participant in the ASD group showed these parameters > 2 SD and was excluded from the group comparison for TD > ASD (FE > NE contrast).

Results

Group comparisons of sex, age, AQ, AASP, and STAI scores are shown in Table 1. There were no significant differences in sex ratio or age between the TD and ASD groups. Individuals with ASD reported higher scores for Low registration, Sensory sensitivity, and Sensation avoiding (AASP) compared with individuals in the TD group, whereas the TD group showed increased Sensation seeking score. Both State and Trait anxiety scores were higher in the ASD group than in the TD group.

Task performance

Estimated JND of the TOJ during the anatomical scan did not differ between the groups (mean JND: TD = 17.20 ms, ASD = 16.58 ms; $t = 0.19$, $df = 47.80$, $p = 0.85$, $d = 0.05$, 95% confidence interval [CI] = [-0.5, 0.61]). We also compared task performance during fMRI between the groups. The GLMM-based ANOVA revealed a main effect of group ($F_{1,48} = 6.36$, $p = 0.015$, partial $\eta^2 = 0.12$) and face condition ($F_{1,48} = 6.89$, $p = 0.01$, partial $\eta^2 = 0.13$), but no group \times face condition interaction ($F_{1,48} = 2.07$, $p = 0.16$, partial $\eta^2 = 0.04$). Post hoc analyses revealed that the TD group showed more correct performances than the ASD group under the FE condition ($p = 0.005$), which was marginally significant under the NE condition ($p = 0.08$). There was a significant departure from zero in the Δ Correct rate (correct performance under the FE condition minus NE condition) in the TD group ($t = 3.87$, $df = 24$, $p < 0.001$, $d = 0.77$, CI = [-1.24, 2.78]), but not in the ASD group ($t = 0.70$, $df = 24$, $p = 0.49$, $d = 0.14$, CI = [-1.86, 2.14], Fig. 2). Presentation of the fear-relevant face image improved TOJ task performance only in the TD group.

Correlations across behavioral data

We examined the association between the emotion effect on the TOJ task and psychological assessments. There was no correlation between the Δ Correct rate and either the State or Trait anxiety scores in the TD group. Because total anxiety (the cumulative score of STAI State and Trait subscales) also reflects threatening and negative emotion conditions, we additionally used this metric as a measure of total anxiety level^{48–51}. Again, no correlation was found between the Δ Correct rate and the total anxiety score in the TD group. The ASD group showed a negative correlation between the Δ Correct rate and the STAI total score ($r = -0.46$, $p = 0.02$, [1 - β] = 0.66, Fig. 3). A trend could be seen in the Δ Correct rate and State anxiety ($r = -0.46$, $p = 0.02$, [1 - β] = 0.66), and a moderate correlation was found between the rate and Trait anxiety ($r = -0.36$, $p = 0.08$, [1 - β] = 0.42). The ASD group also showed positive correlations between AASP hyperreactivity (Sensory sensitivity + Sensation avoiding) and State anxiety ($r = 0.53$, $p = 0.006$, [1 - β] = 0.80), Trait anxiety ($r = 0.53$, $p = 0.006$, [1 - β] = 0.80), and STAI total ($r = 0.60$, $p = 0.002$, [1 - β] = 0.91), respectively. The TD group showed no such associations (p -values > 0.17). Based on the associations across the behavioral indices in the ASD group, we used the STAI total score (State + Trait anxiety scores) as the metric of anxiety level.

fMRI results

Group comparison

We tested the differences in neural correlates between the groups. By comparing the FE > NE contrast with age, sex, and JND as covariates of no interest, we found greater BOLD signals peaking at several coordinates in the TD group compared with the ASD group. Table 2 shows some peak coordinates, where we could clearly define the cortical anatomical location using the atlases (which seemed to be part of the ventricle). We suspected that motion artifacts in the ASD group might have resulted in the idiosyncratic coordinates. We therefore applied a motion outlier test in the ASD participants using ArtRepair toolbox. Based on the outlier test, we excluded one participant with the largest motion artifact across the brain images and carried out the same second level group comparison. The comparison between 25 TD and 24 ASD participants indicated slightly altered coordinates, as shown in Table 2, indicating the right caudate (labeling procedure was explained in “Methods” section).

Multiple regression

We performed whole-brain multiple regression analyses for FE > NE contrast with age and sex as covariates of no interest in each group. No suprathreshold region with positive association with the Δ Correct rate was found in the ASD group. ASD participants showed negative associations between the Δ Correct rate and the bilateral fusiform gyri (the fusiform face area, FFA⁵²; the fourth cluster shown in Table 3; Fig. 4) and the left precentral gyrus (ventral premotor cortex). The TD group showed no significant association of BOLD signals and Δ Correct rate.

We also analyzed the brain regions associated with the psychological assessments for FE > NE contrast (Table 4; Fig. 5 left). We found a positive association between STAI total and the BOLD signal at the right angular gyrus in the ASD group. ASD participants who reported greater AASP hyperreactivity score exhibited increased signal change at the right superior temporal gyrus (Table 5; Fig. 5 right). The cluster of this correlation also involved the right temporal pole, shown as the second coordinate in the table. In the TD group, none of the psychological assessments (STAI and AASP, respectively) were associated with BOLD signal change.

Functional connectivity

We analyzed the functional connectivity for the FE > NE contrast based on the strong assumption for the region involved emotional processing. By using the anatomical mask of the bilateral amygdala as the seed region, we found a psychophysiological interaction with the left supramarginal gyrus (Table 6; Fig. 6). ASD participants showed no suprathreshold coordinate associated with the seed region.

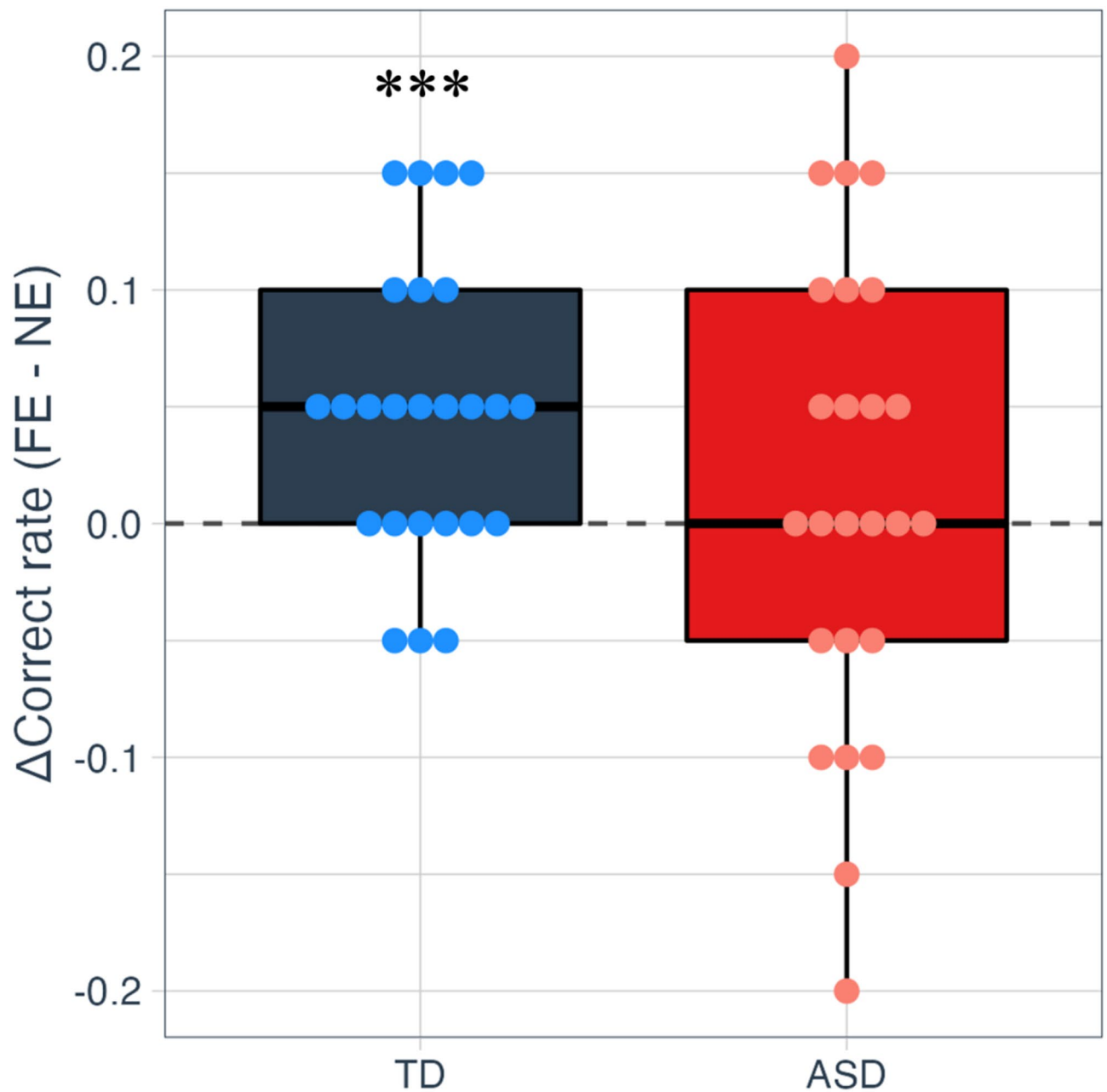


Fig. 2. The effect of fear-relevant image presentation on the TOJ task performance during fMRI. Dots represent the difference of correct rates under the fearful face (FE) minus neutral face (NE) condition (Δ Correct rate) in each participant. *** $p < 0.001$.

Mediation analysis

There was a positive correlation between AASP sensory hyperreactivity score (Sensory sensitivity + Sensation avoiding score) and STAI total score, and a marginally significant association between the BOLD signal change at the right angular gyrus (rAng) and STAI total score ($p_{\text{FWE}} = 0.057$, Table 4; Fig. 5 left) in the ASD group. For the latter relationship, the Pearson's correlation coefficient r between signal change and STAI was 0.74, power $(1 - \beta) = 0.995$, and Bayesian factor $BF_{10} = 1084.87$, indicating a large effect size. We confirmed that the signal change correlating with STAI total score was also positively correlated with the AASP sensory hyperreactivity score ($r = 0.46$, $p = 0.02$, $[1 - \beta] = 0.66$). Since the signal change was correlated with these psychometric parameters, we performed a causal mediation analysis⁴² to determine whether the association predicted sensory hyperreactivity in ASD. As the result, the mediation model was significant, suggesting STAI total score mediated the relationship between the signal change at the rAng and AASP sensory hyperreactivity score (for more details, see [Supplementary Materials](#)).

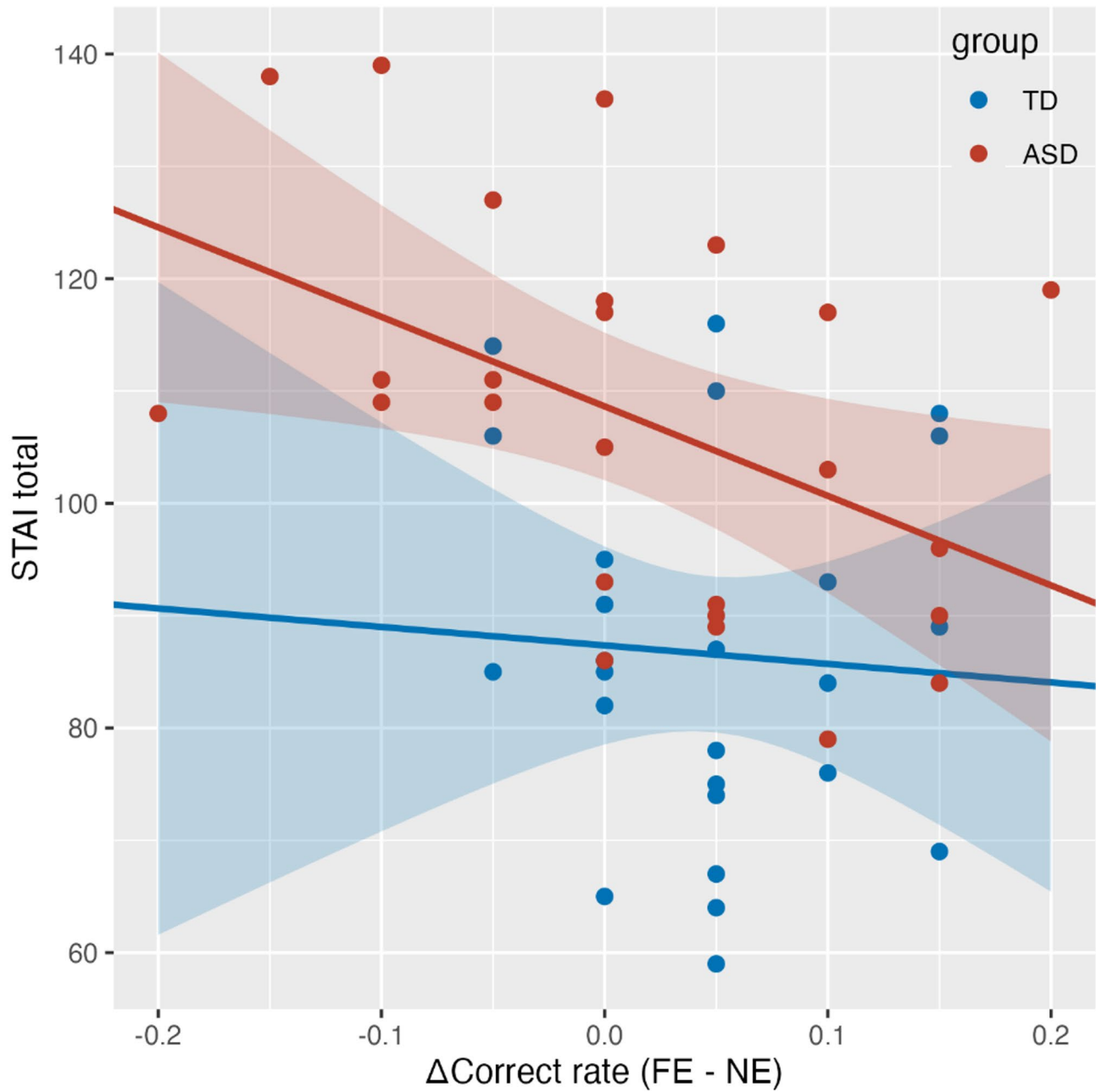


Fig. 3. Correlations between the Δ Correct rate of TOJ performance (FE – NE condition) and the STAI total score in each group. * $p < 0.05$. Shaded area represents 95% confidence interval.

	Size (voxel)	z-value	p_{FWE}	L/R	Region	BA	MNI coordinate		
							x	y	z
TD (25) > ASD (25)	461	5.02	0.001	R	–	–	26	4	26
TD (25) > ASD (24)	408	3.90	0.002	R	Caudate	–	18	22	8

Table 2. Group comparisons for FE > NE contrast. TD: typically developed; ASD: autism spectrum disorder; FWE: family wise error; BA: Brodmann area; MNI: Montreal Neurological Institute.

Group (n)	Size (voxel)	z-value	p _{FWE}	L/R	Region	BA	MNI coordinate		
							x	y	z
ASD (25)	699	4.69	0.000	R	Fusiform gyrus	37	54	- 64	- 2
	403	4.65	0.000	L	Precentral gyrus		- 42	- 2	38
	183	4.06	0.028	L	Fusiform gyrus	37	- 52	- 60	- 2
	211	4.03	0.015	R	Fusiform gyrus	37	36	- 56	- 18

Table 3. Brain regions negatively associated with Δ Correct rate (FE > NE). ASD: autism spectrum disorder; FWE: family wise error; BA: Brodmann area; MNI: Montreal Neurological Institute.

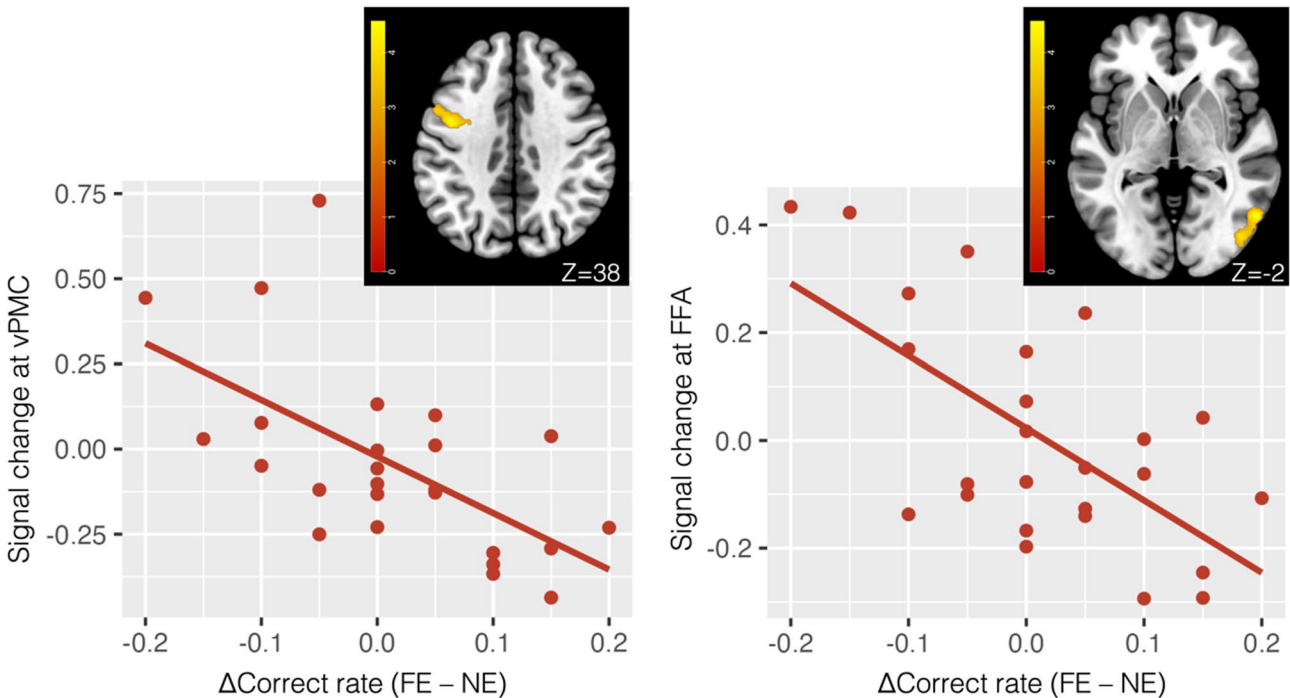


Fig. 4. Correlations of fMRI activation (FE > NE) and Δ Correct rate of TOJ performance (FE – NE condition) in the left ventral premotor cortex (vPMC, left panel) and the right fusiform face area (FFA, right panel) in ASD. Color bars represent the z-values for each SPM signal change (insets).

Group (n)	Size (voxel)	z-value	p _{FWE}	L/R	Region	BA	MNI coordinate		
							x	y	z
ASD (25)	155	4.00	0.057	R	Angular gyrus	39	34	- 82	30

Table 4. Brain regions positively associated with STAI total score (FE > NE). ASD: autism spectrum disorder; FWE: family wise error; BA: Brodmann area; MNI: Montreal Neurological Institute.

Discussion

In the current study, we sought to reveal the common neural circuit for sensory hyperresponsiveness and anxiety level in autism by focusing on improvement of temporal processing of visual stimuli. By cueing a fear-relevant face image, the subsequent task performance of TOJ was improved in the TD group but not in the ASD group. In fact, ASD participants with greater total anxiety score exhibited worse performance under the fear-face condition. Greater BOLD signal, as a proxy of task-related neural activation, was found in a region close to the right caudate in TD participants compared with ASD participants under the fear-face condition. A psychophysiological interaction analysis revealed functional connectivity of the bilateral amygdala and the left supramarginal gyrus in the TD group. This association was absent in the ASD group, in which rAng activity seemingly strengthened their sensory hyperresponsiveness mediated by increased total anxiety. The basal ganglia, an organization of the multiple nuclei including the caudate, is considered essential for timing (see review by⁹). In the TOJ task, the bilateral caudate is activated relative to the numerosity judgment

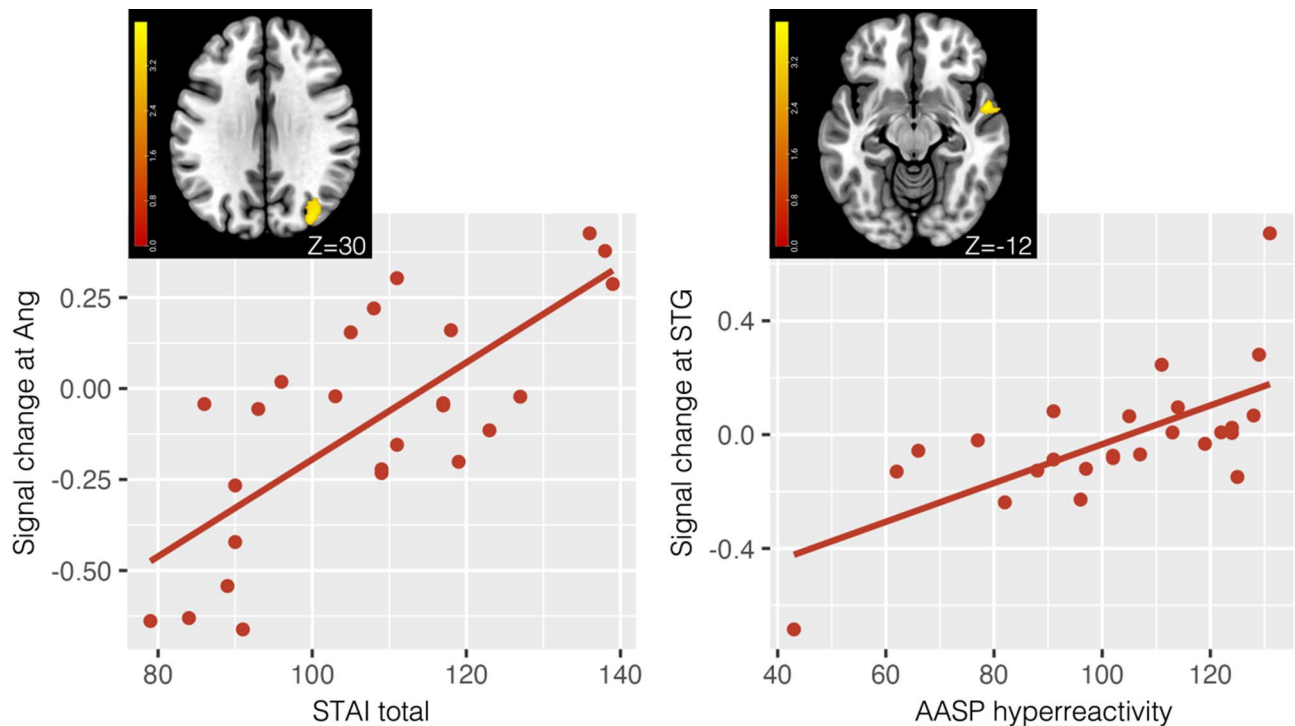


Fig. 5. Correlations of fMRI activation (FE > NE) and the psychological measurements in ASD. *Left:* Association between STAI total score and signal changes in the right angular gyrus (Ang). *Right:* AASP hyperreactivity score and the right superior temporal gyrus (STG). Color bars represent the z-values for each SPM signal change (insets).

Group (n)	Size (voxel)	z-value	p _{FWE}	L/R	Region	BA	MNI coordinate		
							x	y	z
ASD (25)	179	4.30	0.031	R	Superior temporal gyrus	22	56	4	-12
					Temporal pole	38	62	8	-6

Table 5. Brain regions positively associated with AASP hyperreactivity score (FE > NE). ASD: autism spectrum disorder; FWE: family wise error; BA: Brodmann area; MNI: Montreal Neurological Institute.

Group (n)	Size (voxel)	z-value	p _{FWE}	L/R	Region	BA	MNI coordinate		
							x	y	z
TD (25)	217	4.40	0.016	L	Supramarginal gyrus	40	-62	-34	30

Table 6. Brain regions functionally connected with the bilateral amygdala (FE > NE). ASD: autism spectrum disorder; FWE: family wise error; BA: Brodmann area; MNI: Montreal Neurological Institute.

task⁵³. The neural correlates for the TOJ and the simultaneity judgment task involve the basal ganglia, including the caudate⁵⁴, indicating that the caudate is the putative common neural substrate for temporal processing. In our study, presentation of the FE image was involved in the activation of the timing-related region such as the caudate in the TD group. This activation may have led to the improvement in TOJ task performance in the TD group relative to that in the ASD group. A functional connectivity analysis revealed that activation of bilateral amygdala is associated with the left supramarginal gyrus (SMG) in the TD. This suggests that the amygdala–left SMG connectivity may be involved in the heightened task performance induced by the fear-relevant stimulus. During a visual TOJ task, it is known that the bilateral parietal cortices show significant neural activations. There are greater activations in the bilateral temporoparietal junctions (TPJs) and the left SMG during the TOJ than in the shape discrimination task⁵⁵. The left SMG involved in inferior parietal lobule is organized with the right TPJ, dorsolateral prefrontal cortex (DLPFC), and the left medial frontal gyrus during audiovisual asynchrony perception⁵⁶. A study that used the task for collision judgments revealed that the left SMG is involved in

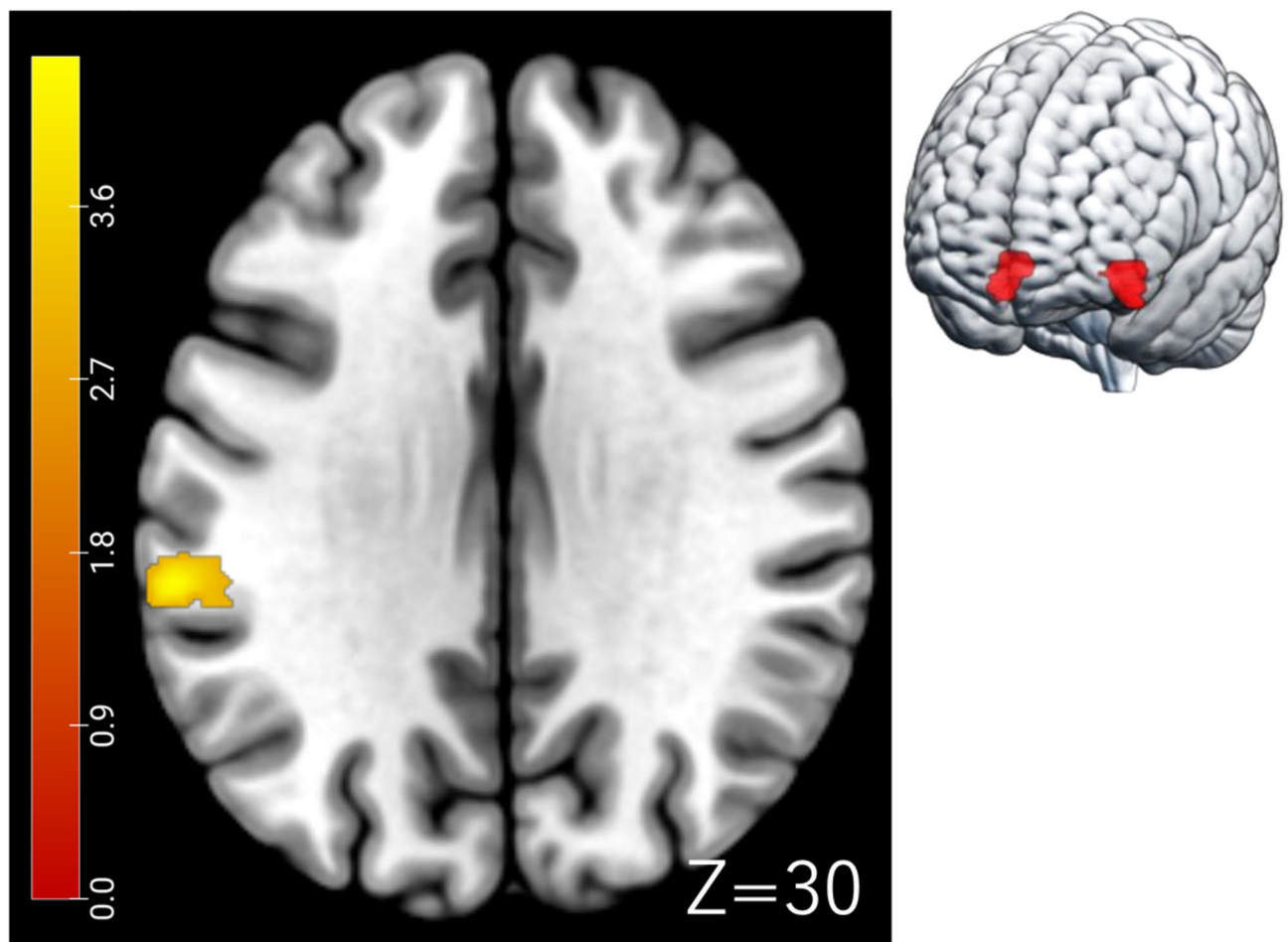


Fig. 6. Psychophysiological interaction (PPI) of the bilateral amygdala as the seed regions (inset) and the left supramarginal gyrus (SMG) for the FE > NE contrast in TD. Color bars represent the z -values for each SPM signal change.

integration of perceptual spatiotemporal information⁵⁷. In the present study, our results suggest that the task-irrelevant fear-face image activated the neural substrate of timing by mediating amygdala activation in the TD group. The nuclei within the amygdala have multiple projections, including the basal ganglia and the inferior parietal cortex⁵⁸. The functional connectivity observed in the TD group might be absent or diminished in the ASD group in our study, suggesting the population-level disrupted connectivity of the neural circuit for timing and emotion driven by fear-relevant cues.

One possibility for the null effect of FE on the TOJ in ASD is that ASD participants were less sensitive to facial expressions. It is evident, however, that individuals with ASD recruit the fusiform gyrus when viewing human face images similar to neurotypical individuals (as shown in a quantitative meta-analysis study⁵⁸). Participants with ASD in the current study who demonstrated better task performance under the FE condition exhibited lower activation of the fusiform gyri, including the fusiform face area (FFA). Activation of the FFA is not sufficient to explain the lack of improvement in task performance in the ASD group. It should be noted that there is broad acceptance of the existence of bidirectional communication between the amygdala and the fusiform gyrus during emotional image viewing^{59,60}. The dissociation of morphological metrics between the amygdala and the FFA may be related to autistic face recognition traits⁶¹. Combining these findings with our results in the ASD group, we can speculate that the presentation of fear-face may disrupt the activation of the amygdala–fusiform circuit and lead to dysregulation of the timing performance.

We also found that autistic participants who exhibited enhanced task performance under the FE relative to the NE condition showed lower anxiety scores. This suggests that a better emotion-control trait may enhance cognitive performance including TOJ by fear-face cue, even in people with ASD. The participants with ASD exhibiting poorer performance under the FE condition tended to show greater activity of the left vPMC, which is thought to be involved in the TOJ task^{36,53,54}. These results suggest that TOJ task performance in ASD might be disrupted by fear-relevant stimulus presentation due to the relatively uncontrollable emotion property. This idea may also be supported by findings that autistic people exhibit similar difficulties to people with amygdala lesions. Both groups show eye avoidance because of the amygdala-related hyperarousal^{62,63}.

We found a potential association between STAI total score and rAng activity in the ASD group. It is broadly accepted that the rAng, part of the inferior parietal lobule (IPL), is also involved in sub-second perceptual timing tasks such as those in our experiment (see a voxel-wise meta-analysis study⁶⁴). The right IPL may be sensitive to sub-second durations^{65–67}. The bilateral angular gyri are also recruited for the time estimation task⁶⁸, and the rAng is involved in the emotion-related time production task⁶⁹. One study showed that the altered functional connectivity between the right DLPFC and the angular gyrus was positively correlated with anxiety severity in generalized anxiety disorders⁷⁰. The right lateralized regions of prefrontal and posterior parietal cortices are considered to constitute a large-scale network for attention⁷¹. In line with previous knowledge of the relationship between pathological anxiety and the fronto-parietal network, we can assume the possibility that the arousal response derived by emotion-present image activated the attention-related brain region relative to the individual anxiety property in the ASD group.

The role of the rAng might be key to understanding sensory hyperreactivity in ASD. The mediation analysis suggested that activation of the rAng was correlated with increase of the sensory hyperreactivity score mediated by total anxiety score. One study showed that the right DLPFC-right angular gyrus association for the anxiety pathology⁷⁰. The neural excitatory/inhibitory (E/I) imbalance in the right TPJ, which is formed by the IPL (the angular gyrus and the SMG), may be associated with sensory hyperresponsiveness in ASD⁷². We speculate that increased attention and arousal cued by an emotion-relevant stimulus derived from activation of this circuit⁷¹ might focus on behaviorally irrelevant sensory stimuli, resulting in autistic sensory over-responsivity in everyday life. We must state that the results of the mediation analysis should be interpreted with great caution because the mediation model is based on a marginally significant association between the rAng and STAI total ($p_{FWE} = 0.057$).

Whole-brain analysis of correlations revealed a positive association between the sensory hyperreactivity score of AASP and the combined regions of the right superior temporal gyrus and temporal pole. The right temporal pole is considered to be involved in emotional face processing⁷³. Increased local functional connectivity in the ASD group in temporo-occipital regions, including the right temporal pole, was correlated with severities of social communication deficits and repetitive and restricted behaviors⁷⁴. Another task-related fMRI study revealed that ASD participants showed greater bilateral temporal pole activations in viewing face-like objects⁷⁵. The presentation of emotion-related face images might elicit the unique brain activation for socioemotional processing relative to an autism symptom; that is, sensory hyperreactivity.

Fear-face presentation did not enhance TOJ performance in ASD, and task improvement was negatively correlated with STAI total score. These results seem in opposition to our previous finding that disgust-face improved TOJ temporal resolution in ASD¹⁷. A literature review indicated that disgust evokes activation of the anterior insula, whereas fear leads to activation of the amygdala¹⁹. Previous research demonstrated that aberrant but distinguishable functional characteristics of the insula⁷⁶ and amygdala⁶⁰ exist in ASD, consistent with its pathology. In TDs, a disgusting image more efficiently captures attention⁷⁷ and impairs subsequent cognitive control⁷⁸ to a greater extent than fearful images. In the present study, absence or diminished functional connectivity of the amygdala in the ASD participants suggested a null effect of the fear-face image on our task. Considering a previous study showing that disgust face image had equivalent efficacy for attentional bias in the ASD and TD individuals⁷⁹, we speculate that impairment in cognitive control by disgust and increased arousal by fear face are reduced in ASD.

In line with the hypothesis that increased sensory processing precision may lead to daily sensory over-reactivity in autism^{12,13,36}, we examined the effect of fear-relevant image presentation on timing performance. This is based on the idea that emotion dysregulation would increase both the precision of sensory processing and daily sensory challenges. In contrast to our hypothesis, we observed improvement of temporal processing precision in TD but not ASD participants. The individuals with ASD who showed task improvement under the fear-face condition exhibited reduced activation of the vPMC, which is considered to be involved in TOJ performance^{36,53,54}. Because we used the subtraction method between the FE and NE conditions, we assumed that the effect of handedness and motion in each condition on the vPMC and motor cortex imaging data would be canceled out. We previously reported that GABA concentration in the left vPMC was negatively correlated with AASP hyperreactivity scores in ASD¹⁰. The neural E/I imbalance is suggested to be the therapeutic target in autism pathophysiology^{80,81}. It is suggested that the neural excitability of this region may contribute to timing precision and daily sensory challenges in autism. The present finding of the emotion effect on the TOJ performance in ASD implies that separate mechanisms may exist to increase the precision of sensory processing and daily sensory challenges. Our data, however, suggest that emotion dysregulation (i.e., increased anxiety) may enhance the daily sensory challenges induced by the neural response of the region involved in timing and attention control under negative emotion situations.

In the present study, we attempted to potentially evoke the affective states by the task-irrelevant face image and examined its effect on the TOJ. It remains unknown how task-relevant stimuli eliciting stressful or negative emotional response work on timing precision in individuals with ASD. Future studies should address this point, as well as the relationship with daily sensory challenges. Separate MR spectroscopy analysis may reveal how E/I imbalance is involved in sensory processing precision and sensory abnormalities in autism.

Limitations and future directions

The current study has some limitations. Increased arousal may influence general cognitive performance not specific to timing perception. So far, it is difficult to conclude that the improvement in TOJ task performance in the TD group was equivalent to that observed in ASD¹⁷. For future studies, further experiments should be conducted to examine the comparison between timing tasks and other cognitive domains (e.g., numerosity judgment^{36,53}) and involvement of the rAng in relation to sensory issues in ASD. Another weakness of our study may be the missing IQ data. We did not assess IQ scores in the TD group, but only screened for the presence of

a clinical diagnosis of mental retardation. In our data, the differences in task performance without face image presentation and the correct rate in the NE condition between groups were not significant. We speculated that IQ scores did not affect task comprehension or the difference in task performance without emotional valence (i.e., fear face presentation). The finding that TOJ task performance in individuals with ASD is equivalent to that in individuals without ASD was consistent with previous studies^{17,36}. However, the lack of IQ data in the control group limits our ability to claim that IQ score had no effect on the group differences for the fear face presentation in the present study. Future studies should address the impact of intellectual ability on the neural correlates of emotion-induced cognitive performance in ASD. Further, the effect of the face image set may not be ignorable. We used two sets of face images depicting non-Japanese subjects. A previous study examined the difference in BOLD signal changes associated with the presentation of fearful faces between Japanese and Caucasian people living in the United States⁸². The authors found that the increased amygdala response to fear faces of one's own cultural region was independent of the racial difference of the participants. This suggests that a race- or culture-specific response to the fear face image was present but a response to the other racial faces was not. This culture-specific effect may explain why we did not find increased signal change in the amygdala in the control group. Future studies should address the race- or culture-specific response of the amygdala during our task. Discussion of our exclusion protocol is also warranted. For the group-level comparison, we employed the ArtRepair toolbox to detect an outlier based on the a priori knowledge that imaging data from ASD participants may be blurred by motion due to abnormal motor functions³⁷. Therefore, we performed outlier detection only for the ASD group. However, we recognize that the outlier detection is usually done for all groups and that this could introduce a bias in this study.

Data availability

The datasets generated for this study are available on request to the corresponding author.

Received: 26 September 2024; Accepted: 12 May 2025

Published online: 21 May 2025

References

- Tomchek, S. D. & Dunn, W. Sensory processing in children with and without autism: a comparative study using the short sensory profile. *Am. J. Occup. Ther.* **61**, 190–200 (2007). <http://www.ncbi.nlm.nih.gov/pubmed/17436841>
- Nimmo-Smith, V. et al. Anxiety disorders in adults with autism spectrum disorder: a Population-Based study. *J. Autism Dev. Disord.* **50**, 308–318. <https://doi.org/10.1007/s10803-019-04234-3> (2020).
- Vasa, R. A., Keefer, A., McDonald, R. G., Hunsche, M. C. & Kerns, C. M. A scoping review of anxiety in young children with autism spectrum disorder. *Autism Res.* **13**, 2038–2057. <https://doi.org/10.1002/aur.2395> (2020).
- Roelofs, K. Freeze for action: neurobiological mechanisms in animal and human freezing. *Philos. Trans. R Soc. Lond. B Biol. Sci.* **372**, 20160206. <https://doi.org/10.1098/rstb.2016.0206> (2017).
- Green, S. A. et al. Distinct patterns of neural habituation and generalization in children and adolescents with autism with low and high sensory overresponsivity. *Am. J. Psychiatry.* **176**, 1010–1020. <https://doi.org/10.1176/appi.ajp.2019.18121333> (2019).
- Jung, J. et al. Associations between physiological and neural measures of sensory reactivity in youth with autism. *J. Child. Psychol. Psychiatry.* **62**, 1183–1194. <https://doi.org/10.1111/jcpp.13387> (2021).
- MacLennan, K., Roach, L. & Tavassoli, T. The relationship between sensory reactivity differences and anxiety subtypes in autistic children. *Autism Res.* **13**, 785–795. <https://doi.org/10.1002/aur.2259> (2020).
- Pickard, H., Hirsch, C., Simonoff, E. & Happé, F. Exploring the cognitive, emotional and sensory correlates of social anxiety in autistic and neurotypical adolescents. *J. Child. Psychol. Psychiatry.* **61**, 1317–1327. <https://doi.org/10.1111/jcpp.13214> (2020).
- Buhusi, C. V. & Meck, W. H. What makes Us tick? Functional and neural mechanisms of interval timing. *Nat. Rev. Neurosci.* **6**, 755–765. <https://doi.org/10.1038/nrn1764> (2005).
- Umesawa, Y., Atsumi, T., Chakrabarty, M., Fukatsu, R. & Ide, M. GABA concentration in the left ventral premotor cortex associates with sensory hyperresponsiveness in autism spectrum disorders without intellectual disability. *Front. Neurosci.* **14**, 482. <https://doi.org/10.3389/fnins.2020.00482> (2020).
- Wood, E. T. et al. Sensory over-responsivity is related to GABAergic Inhibition in thalamocortical circuits. *Trans. Psychiatry.* **11**, 39. <https://doi.org/10.1038/s41398-020-01154-0> (2021).
- Ide, M., Yaguchi, A., Sano, M., Fukatsu, R. & Wada, M. Higher tactile Temporal resolution as a basis of hypersensitivity in individuals with autism spectrum disorder. *J. Autism Dev. Disord.* **49**, 44–53. <https://doi.org/10.1007/s10803-018-3677-8> (2019).
- Kaneko, A., Atsumi, T. & Ide, M. Temporal resolution relates to sensory hyperreactivity independently of stimulus detection sensitivity in individuals with autism spectrum disorder. *Perception* **53**, 585–596. https://doi.org/10.1007/978-1-4614-6435-8_102347-1 (2024).
- Schulz, S. E. & Stevenson, R. A. Sensory hypersensitivity predicts repetitive behaviours in autistic and typically-developing children. *Autism* **23**, 1028–1041. <https://doi.org/10.1177/1362361318774559> (2019).
- Allman, M. J. & Meck, W. H. Pathophysiological distortions in time perception and timed performance. *Brain* **135** (3), 656–677. <https://doi.org/10.1093/brain/awr210> (2012).
- Meilleur, A., Foster, N. E. V., Coll, S. M., Brambati, S. M. & Hyde, K. L. Unisensory and multisensory Temporal processing in autism and dyslexia: a systematic review and meta-analysis. *Neurosci. Biobehav. Rev.* **116**, 44–63. <https://doi.org/10.1016/j.neubiorev.2020.06.013> (2020).
- Chakrabarty, M., Atsumi, T., Kaneko, A., Fukatsu, R. & Ide, M. State anxiety modulates the effect of emotion cues on visual Temporal sensitivity in autism spectrum disorder. *Eur. J. Neurosci.* **54**, 4682–4694. <https://doi.org/10.1111/ejn.15311> (2021).
- Adolphs, R. Fear, faces, and the human amygdala. *Curr. Opin. Neurobiol.* **18**, 166–172. <https://doi.org/10.1016/j.conb.2008.06.006> (2008).
- Cisler, J. M., Olatunji, B. O. & Lohr, J. M. Disgust, fear, and the anxiety disorders: a critical review. *Clin. Psychol. Rev.* **29**, 34–46. <https://doi.org/10.1016/j.cpr.2008.09.007> (2009).
- Bzdok, D., Laird, A. R., Zilles, K., Fox, P. T. & Eickhoff, S. B. An investigation of the structural, connectional, and functional subspecialization in the human amygdala. *Hum. Brain Mapp.* **34**, 3247–3266. <https://doi.org/10.1002/hbm.22138> (2013).
- Japanese, W. A. I. S. I. I. & Publication Committee. *Japanese Wechsler Adult Intelligence Scale-Third Edition Tokyo* (Nihon Bunka Kagakusya, 2006).
- Japanese, W. I. S. C. I. I. I. Publication Committee. *Nihonban WISC-III Chinou Kenshou* (Japanese Wechsler Intelligence Scale for Children) 3rd edition. Tokyo: Nihon Bunka Kagakusya (1998).

23. Baron-Cohen, S., Wheelwright, S., Skinner, R., Martin, J. & Clubley, E. The autism-spectrum quotient (AQ): evidence from asperger syndrome/high-functioning autism, males and females, scientists and mathematicians. *J. Autism Dev. Disord.* **31**, 5–17 (2001). <http://www.ncbi.nlm.nih.gov/pubmed/11439754>
24. Wakabayashi, A., Tojo, Y., Baron-Cohen, S. & Wheelwright, S. The Autism-Spectrum quotient (AQ) Japanese versions: evidence from high-functioning clinical group and normal adults. *Jpn J. Psychol.* **75**, 78–84. <https://doi.org/10.4992/jjpsy.75.78> (2004).
25. Brown, C., Tollefson, N., Dunn, W., Cromwell, R. & Filion, D. The adult sensory profile: measuring patterns of sensory processing. *Am. J. Occup. Ther.* **55**, 75–82. <https://doi.org/10.5014/ajot.55.1.75> (2001).
26. Dunn, W. The impact of sensory processing abilities on the daily lives of young children and their families: a conceptual model. *Infants Young Child.* **9**, 23–35. <https://doi.org/10.1097/00001163-199704000-00005> (1997).
27. Ayres, J. *Sensory Integration and the Child Understanding Hidden Sensory Challenges* (Western Psychological Services, 1979).
28. Dunn, W. The sensations of everyday life: empirical, theoretical, and pragmatic considerations. *Am. J. Occup. Ther.* **55**, 608–620. <https://doi.org/10.5014/ajot.55.6.608> (2001).
29. Spielberger, C. D., Gorsuch, R. L., Lushene, R., Vagg, P. R. & Jacobs, G. A. *State-Trait Anxiety Inventory for Adults — Manual, Instrument and Scoring Guide* (Consulting Psychologists Press, 1983). <https://doi.org/10.1037/106496-000>.
30. Iwamoto, M. et al. A study of the state-trait anxiety inventory (STAI) and its application to noise stress. *Nippon Eiseigaku Zasshi (Japanese J. Hygiene)*. **43**, 1116–1123. <https://doi.org/10.1265/jjh.43.1116> (1989).
31. Peirce, J. et al. PsychoPy2: experiments in behavior made easy. *Behav. Res. Methods*. **51**, 195–203. <https://doi.org/10.3758/s13428-018-01193-y> (2019).
32. Tottenham, N. et al. The nimstim set of facial expressions: judgments from untrained research participants. *Psychiatry Res.* **168**, 242–249. <https://doi.org/10.1016/j.psychres.2008.05.006> (2009).
33. van der Schalk, J., Hawk, S. T., Fischer, A. H. & Doosje, B. Moving faces, looking places: validation of the Amsterdam dynamic facial expression set (ADFES). *Emotion* **11**, 907–920. <https://doi.org/10.1037/a0023853> (2011).
34. Wingenbach, T. S. H., Ashwin, C. & Brosnan, M. Validation of the Amsterdam dynamic facial expression set – Bath intensity variations (ADFES-BIV): A set of videos expressing low, intermediate, and high intensity emotions. *PLoS One*. **11**, e0147112. <https://doi.org/10.1371/journal.pone.0147112> (2016).
35. Ogawa, S. et al. Functional brain mapping by blood oxygenation level-dependent contrast magnetic resonance imaging. A comparison of signal characteristics with a biophysical model. *Biophys. J.* **64** (3), 803–812. [https://doi.org/10.1016/S0006-3495\(93\)81441-3](https://doi.org/10.1016/S0006-3495(93)81441-3) (1993).
36. Ide, M. et al. Neural basis of extremely high Temporal sensitivity: insights from a patient with autism. *Front. Neurosci.* **14**, 340. <https://doi.org/10.3389/fnins.2020.00340> (2020).
37. Nebel, M. B. et al. Accounting for motion in resting-state fMRI: What part of the spectrum are we characterizing in autism spectrum disorder? *Neuroimage* **257**, 119296. <https://doi.org/10.1016/j.neuroimage.2022.119296> (2022).
38. O'Reilly, J. X., Woolrich, M. W., Behrens, T. E. J., Smith, S. M. & Johansen-Berg, H. Tools of the trade: psychophysiological interactions and functional connectivity. *Soc. Cogn. Affect. Neurosci.* **7**, 604–609. <https://doi.org/10.1093/scan/nss055> (2012).
39. Maldjian, J. A., Laurienti, P. J., Kraft, R. A. & Burdette, J. H. An automated method for neuroanatomic and cytoarchitectonic atlas-based interrogation of fMRI data sets. *Neuroimage* **19**, 1233–1239. [https://doi.org/10.1016/S1053-8119\(03\)00169-1](https://doi.org/10.1016/S1053-8119(03)00169-1) (2003).
40. Maldjian, J. A., Laurienti, P. J. & Burdette, J. H. Precentral gyrus discrepancy in electronic versions of the Talairach atlas. *Neuroimage* **21**, 450–455. <https://doi.org/10.1016/j.neuroimage.2003.09.032> (2004).
41. Tzourio-Mazoyer, N. et al. Automated anatomical labeling of activations in SPM using a macroscopic anatomical parcellation of the MNI MRI single-subject brain. *Neuroimage* **15**, 273–289. <https://doi.org/10.1006/nimg.2001.0978> (2002).
42. Baron, R. M. & Kenny, D. A. The moderator–mediator variable distinction in social psychological research: conceptual, strategic, and statistical considerations. *J. Pers. Soc. Psychol.* **51**, 1173–1182. <https://doi.org/10.1037/0022-3514.51.6.1173> (1986).
43. Tingley, D., Yamamoto, T., Hirose, K., Keele, L. & Imai, K. Mediation: R package for causal mediation analysis. *J. Stat. Softw.* **59**, 145. <https://doi.org/10.18637/jss.v059.i05> (2014).
44. Eickhoff, S. B. et al. A new SPM toolbox for combining probabilistic cytoarchitectonic maps and functional imaging data. *Neuroimage* **25**, 1325–1335. <https://doi.org/10.1016/j.neuroimage.2004.12.034> (2005).
45. Lacadie, C. M., Fulbright, R. K., Rajeevan, N., Constable, R. T. & Papademetris, X. More accurate Talairach coordinates for neuroimaging using non-linear registration. *NeuroImage* **42**, 717–725. <https://doi.org/10.1016/j.neuroimage.2008.04.240> (2008).
46. Washington, S. D. et al. Dysmaturation of the default mode network in autism. *Hum. Brain Mapp.* **35**, 1284–1296. <https://doi.org/10.1002/hbm.22252> (2014).
47. Mazaika, P. K., Hoeff, F., Glover, G. H. & Reiss, A. L. Methods and software for fMRI analysis of clinical subjects. *NeuroImage* **47**, 56. [https://doi.org/10.1016/S1053-8119\(09\)70238-1](https://doi.org/10.1016/S1053-8119(09)70238-1) (2009).
48. Calik Koseler, B., Yilanci, H. & Ramoglu, S. I. Does audiovisual information affect anxiety and perceived pain levels in Miniscrew application? — a within-person randomized controlled trial. *Prog. Orthod.* **20**, 29. <https://doi.org/10.1186/s40510-019-0281-1> (2019).
49. Sorribes De Ramón, L. A. et al. Effect of virtual reality and music therapy on anxiety and perioperative pain in surgical extraction of impacted third molars. *J. Am. Dent. Assoc.* **154**, 206–214. <https://doi.org/10.1016/j.adaj.2022.11.008> (2023).
50. Veeraboina, N. et al. Association of state and trait anxiety with oral health status among adult dental patients. *Acta Biomed.* **91**, e2020070. <https://doi.org/10.23750/abm.v91i3.8986> (2020).
51. Wang, Y., Huang, X. & Liu, Z. The effect of preoperative health education, delivered as animation videos, on postoperative anxiety and pain in femoral fractures. *Front. Psychol.* **13**, 881799. <https://doi.org/10.3389/fpsyg.2022.881799> (2022).
52. Schobert, A. K., Corradi-Dell'Acqua, C., Frühholz, S., van der Zwaag, W. & Vuilleumier, P. Functional organization of face processing in the human superior Temporal sulcus: a 7T high-resolution fMRI study. *Soc. Cogn. Affect. Neurosci.* **13**, 102–113. <https://doi.org/10.1093/scan/nsx119> (2018).
53. Takahashi, T., Kansaku, K., Wada, M., Shibuya, S. & Kitazawa, S. Neural correlates of tactile Temporal-Order judgment in humans: an fMRI study. *Cereb. Cortex.* **23**, 1952–1964. <https://doi.org/10.1093/cercor/bhs179> (2013).
54. Miyazaki, M. et al. Dissociating the neural correlates of tactile Temporal order and simultaneity judgements. *Sci. Rep.* **6**, 23323. <https://doi.org/10.1038/srep23323> (2016).
55. Davis, B., Christie, J. & Rorden, C. Temporal order judgments activate Temporal parietal junction. *J. Neurosci.* **29**, 3182–3188. <https://doi.org/10.1523/JNEUROSCI.5793-08.2009> (2009).
56. Adhikari, B. M., Goshorn, E. S., Lamichhane, B. & Dhamala, M. Temporal-Order judgment of audiovisual events involves network activity between parietal and prefrontal cortices. *Brain Connect.* **3**, 536–545. <https://doi.org/10.1089/brain.2013.0163> (2013).
57. Assmus, A. et al. Left inferior parietal cortex integrates time and space during collision judgments. *Neuroimage* **20**, S82–S88. <https://doi.org/10.1016/j.neuroimage.2003.09.025> (2003).
58. Ammons, C. J., Winslett, M. E. & Kana, R. K. Neural responses to viewing human faces in autism spectrum disorder: A quantitative meta-analysis of two decades of research. *Neuropsychologia* **150**, 107694. <https://doi.org/10.1016/j.neuropsychologia.2020.107694> (2021).
59. Frank, D. W., Costa, V. D., Averbeck, B. B. & Sabatinelli, D. Directional interconnectivity of the human amygdala, fusiform gyrus, and orbitofrontal cortex in emotional scene perception. *J. Neurophysiol.* **122**, 1530–1537. <https://doi.org/10.1152/jn.00780.2018> (2019).
60. Herrington, J. D., Taylor, J. M., Grupe, D. W., Curby, K. M. & Schultz, R. T. Bidirectional communication between amygdala and fusiform gyrus during facial recognition. *Neuroimage* **56**, 2348–2355. <https://doi.org/10.1016/j.neuroimage.2011.03.072> (2011).

61. Dziobek, I., Bahnemann, M., Convit, A. & Heekeren, H. R. The role of the Fusiform-Amygdala system in the pathophysiology of autism. *Arc Gen. Psychiatry*. **67**, 397. <https://doi.org/10.1001/archgenpsychiatry.2010.31> (2010).
62. Stuart, N., Whitehouse, A., Palermo, R., Bothe, E. & Badcock, N. Eye gaze in autism spectrum disorder: a review of neural evidence for the eye avoidance hypothesis. *J. Autism Dev. Disord.* **53**, 1884–1905. <https://doi.org/10.1007/s10803-022-05443-z> (2023).
63. Spezio, M. L., Huang, P. Y., Castelli, F. & Adolphs, R. Amygdala damage impairs eye contact during conversations with real people. *J. Neurosci.* **27**, 3994–3997. <https://doi.org/10.1523/JNEUROSCI.3789-06.2007> (2007).
64. Wiener, M., Turkeltaub, P. & Coslett, H. B. The image of time: a voxel-wise meta-analysis. *Neuroimage* **49**, 1728–1740. <https://doi.org/10.1016/j.neuroimage.2009.09.064> (2010).
65. Hayashi, M. et al. Time adaptation shows duration selectivity in the human parietal cortex. *PLoS Biol.* **13**, e1002262. <https://doi.org/10.1371/journal.pbio.1002262> (2015).
66. Hayashi, M., van der Zwaag, W., Bueti, D. & Kanai, R. Representations of time in human frontoparietal cortex. *Commun. Biol.* **1**, 233. <https://doi.org/10.1038/s42003-018-0243-z> (2018).
67. Hayashi, M. & Ivry, R. B. Duration selectivity in right parietal cortex reflects the subjective experience of time. *J. Neurosci.* **40**, 7749–7758. <https://doi.org/10.1523/JNEUROSCI.0078-20.2020> (2020).
68. Morillon, B., Kell, C. A. & Giraud, A. L. Three stages and four neural systems in time Estimation. *J. Neurosci.* **29**, 14803–14811. <https://doi.org/10.1523/JNEUROSCI.3222-09.2009> (2009).
69. Ballotta, D., Lui, F., Porro, C. A., Nichelli, P. F. & Benuzzi, F. Modulation of neural circuits underlying Temporal production by facial expressions of pain. *PLoS One*. **13**, e0193100. <https://doi.org/10.1371/journal.pone.0193100> (2018).
70. Li, W. et al. Specific and common functional connectivity deficits in drug-free generalized anxiety disorder and panic disorder: a data-driven analysis. *Psychiatry Res.* **319**, 114971. <https://doi.org/10.1016/j.psychres.2022.114971> (2023).
71. Boukrina, O. & Barrett, A. M. Disruption of the ascending arousal system and cortical attention networks in post-stroke delirium and Spatial neglect. *Neurosci. Biobehav. Rev.* **83**, 1–10. <https://doi.org/10.1016/j.neubiorev.2017.09.024> (2017).
72. Pierce, S. et al. Associations between sensory processing and electrophysiological and neurochemical measures in children with ASD: an EEG-MRS study. *J. Neurodev. Disord.* **13**, 5. <https://doi.org/10.1186/s11689-020-09351-0> (2021).
73. Olson, I. R., Plotzker, A. & Ezzyat, Y. The enigmatic Temporal pole: a review of findings on social and emotional processing. *Brain* **130**, 1718–1731. <https://doi.org/10.1093/brain/awm052> (2007).
74. Keown, C. L. et al. Local functional overconnectivity in posterior brain regions is associated with symptom severity in autism spectrum disorders. *Cell. Rep.* **5**, 567–572. <https://doi.org/10.1016/j.celrep.2013.10.003> (2013).
75. Hadjikhani, N. & Åsberg Johnels, J. Overwhelmed by the man in the Moon?? Pareidolic objects provoke increased amygdala activation in autism. *Cortex* **164**, 144–151. <https://doi.org/10.1016/j.cortex.2023.03.014> (2023).
76. Nomi, J. S., Molnar-Szakacs, I. & Uddin, L. Q. Insular function in autism: update and future directions in neuroimaging and interventions. *Prog Neuropsychopharmacol. Biol. Psychiatry*. **89**, 412–426. <https://doi.org/10.1016/j.pnpbp.2018.10.015> (2019).
77. Carretié, L., Ruiz-Padial, E., López-Martín, S. & Albert, J. Decomposing unpleasantness: differential exogenous attention to disgusting and fearful stimuli. *Biol. Psychol.* **86**, 247–253. <https://doi.org/10.1016/j.biopsycho.2010.12.005> (2011).
78. Xu, M. et al. The divergent effects of fear and disgust on inhibitory control: an ERP study. *PLoS One*, **10**.
79. Zhao, X., Zhang, P., Fu, L. & Maes, J. H. R. Attentional biases to faces expressing disgust in children with autism spectrum disorders: an exploratory study. *Sci. Rep.* **6**, 19381. <https://doi.org/10.1038/srep19381> (2016).
80. Cellot, G. & Cherubini, E. GABAergic signaling as therapeutic target for autism spectrum disorders. *Front. Pediatr.* **2**, 70. <https://doi.org/10.3389/fped.2014.00070> (2014).
81. Rubenstein, J. L. R. & Merzenich, M. M. Model of autism: increased ratio of excitation/inhibition in key neural systems. *Genes Brain Behav.* **2**, 255–267 (2003).
82. Chiao, J. Y. et al. Cultural specificity in amygdala response to fear faces. *J. Cogn. Neurosci.* **20** (12), 2167–2174. <https://doi.org/10.1162/jocn.2008.20151> (2008).

Acknowledgements

We thank A. Saito, Y. Nakajima, Y. Chida, and Y. Aoki for technical assistance.

Author contributions

TA, MI, and MC conceived the study and designed the experiment. TA prepared the experimental program, partially participated in data collection, analyzed the data, and wrote the manuscript. MI conducted all the experiments. All authors contributed to interpreting the results, reading of the manuscript, providing relevant inputs, and approving the final version of the same.

Funding

This study was supported by MEXT KAKENHI (Grant Number JP18H05523 awarded to Y.T. and JP24H01558 to T.A.), JSPS KAKENHI (JP20K14262 and JP23K03017 awarded to T.A.), and Meiji Yasuda Mental Health Foundation (2021) (awarded to T.A.).

Competing interests

The authors declare no competing interests.

Ethics approval

This study was reviewed and approved by the ethics committee of Kyorin University and the National Rehabilitation Center for Persons with Disabilities. This study was carried out in accordance with the Declaration of Helsinki and the guidelines for human research of both institutes. Written informed consent to participate in this study was provided by the participants themselves. Written informed consent was obtained from the individual(s) for publication of any potentially identifiable images or data included in this manuscript.

Additional information

Supplementary Information The online version contains supplementary material available at <https://doi.org/10.1038/s41598-025-02117-5>.

Correspondence and requests for materials should be addressed to T.A.

Reprints and permissions information is available at www.nature.com/reprints.

Publisher's note Springer Nature remains neutral with regard to jurisdictional claims in published maps and institutional affiliations.

Open Access This article is licensed under a Creative Commons Attribution-NonCommercial-NoDerivatives 4.0 International License, which permits any non-commercial use, sharing, distribution and reproduction in any medium or format, as long as you give appropriate credit to the original author(s) and the source, provide a link to the Creative Commons licence, and indicate if you modified the licensed material. You do not have permission under this licence to share adapted material derived from this article or parts of it. The images or other third party material in this article are included in the article's Creative Commons licence, unless indicated otherwise in a credit line to the material. If material is not included in the article's Creative Commons licence and your intended use is not permitted by statutory regulation or exceeds the permitted use, you will need to obtain permission directly from the copyright holder. To view a copy of this licence, visit <http://creativecommons.org/licenses/by-nc-nd/4.0/>.

© The Author(s) 2025